

# Controlling the Band Gap in Zigzag Graphene Nanoribbons with an Electric Field Induced by a Polar Molecule

Sergio D. Dalosto<sup>\*,†,‡</sup> and Zachary H. Levine<sup>‡</sup>

Department of Physics, University of Washington, Seattle, Washington 98195-1560, and National Institute of Standards and Technology, Gaithersburg, Maryland 20899-8410

Received: December 6, 2007; Revised Manuscript Received: March 6, 2008

Graphene nanoribbons with both armchair- and zigzag-shaped hydrogen-passivated edges (AGNR and ZGNR) have band gaps which depend on the width of the ribbon. In particular, a ZGNR has localized electronic states at the edge which decay exponentially toward the center of the ribbon. Interestingly, application of a uniform external electric field ( $E_{\text{ext}}$ ) in the direction perpendicular to the edge of a ZGNR is capable of reducing the band gap for one spin state ( $\beta$ ) and opens the other spin state ( $\alpha$ ). Moreover, for a critical  $E_{\text{ext}}$  the ZGNR becomes half-metallic. In the case of an 8-chain zigzag ribbon, the critical  $E_{\text{ext}}$  is 2 V/nm within the local spin density approximation. Motivated by these findings, we study the influence on the gap of the electric field produced by a polar ad-molecule to the surface of an 8-zigzag ribbon. The formula units of the ad-molecules that we studied are  $\text{NH}_3(\text{CH})_6\text{CO}_2$  and  $\text{NH}_3(\text{CH})_{10}\text{CO}_2$ . We show that within the generalized gradient approximation the band gap of 0.52 eV without ad-molecule is reduced to 0.27 eV for the  $\beta$ -spin state and increased to 0.69 eV for the  $\alpha$ -spin state. Also, combining the ad-molecule and  $E_{\text{ext}} = 1$  V/nm parallel to the dipole moment of the ad-molecule induces a reduction of the  $\beta$ -spin band gap and an increase for the  $\alpha$ -spin band gap. For  $E_{\text{ext}} = -1$  V/nm, antiparallel to the dipole moment of the ad-molecule, the band gap for both spin states is similar to the case without ad-molecule and  $E_{\text{ext}}$ . These results suggest possible uses for the graphene nanoribbons as sensors or switching devices.

The search for methods to design nanodevices employing spin-selective semiconductors and half metals is the subject of intense investigation. Among the possible materials for nanodevices, graphene<sup>1</sup> is opening new avenues both experimentally and theoretically.<sup>2–7</sup> In particular, a zigzag graphene nanoribbon (ZGNR) is a monolayer of carbon atoms in a two-dimensional honeycomb lattice with hydrogen-terminated edges. It has a gap which depends on the inverse of the width  $w$  of the ribbon.<sup>2–4</sup> In  $n$ -ZGNR ( $n \leq 32$ , where  $n$  is the number of zigzag chains) the ground state is described as ferromagnetically coupled spins at the edges with antiferromagnetic coupling across opposite edges. Recently, a theoretical study showed that in a ZGNR it is possible to tailor the band gap by application of a uniform external electric field perpendicular to the edges.<sup>7</sup> Interestingly, the band gap for  $\alpha$ -spin electrons responds to the electric field perpendicular to the edges oppositely to the  $\beta$ -spin electrons; when the  $\alpha$ -spin gap increases, the  $\beta$  spin decreases. If the  $\beta$  spin closes, the graphene nanoribbon is half metallic with the spin axis normal to the plane of the graphene, which opens the possibility of making devices which exploit that property.

In this work, we study how the band gap of a ZGNR is affected by the presence of polar molecules adsorbed on the surface of the ribbon. Selection of the polar molecules was based on their dipole moments. We believe the results will be representative of a ZGNR with polar molecules.

In this study we consider a ZGNR with eight zigzag chains (8-ZGNR) in a supercell of seven, six, or four subunits, see Figure 1a, and with the edges passivated with hydrogen atoms.

The width for an 8-ZGNR is 1.56 nm excluding the hydrogen atoms. The width of the ribbon was selected considering the computational cost and objective of the present study. We think that increasing the width of the ribbons would lead to the same qualitative results as presented in the present work. Two ad-molecules are used to investigate the effect on the band gap of the ribbon with formula units  $\text{NH}_3(\text{CH})_6\text{CO}_2$  and  $\text{NH}_3(\text{CH})_{10}\text{CO}_2$ . Their dipole moments are  $83 \times 10^{-30}$  (25 Debye) and  $127 \times 10^{-30}$  C m (38 Debye), respectively (1 Debye  $\equiv 10^{-18}$  esu cm  $\equiv 3.33564 \times 10^{-30}$  C m). Hereafter, we will refer to these molecules as short and long ad-molecules. The dipole moment in these molecules is almost along their longitudinal axis. The  $\text{NH}_3$  group is positively charged, while the  $\text{CO}_2$  moiety is negatively charged, but overall the molecules are neutral. These molecules were chosen based on their large dipole moment and size with respect to the width of the ribbon. The ribbon with the short ad-molecule is shown in Figure 1 in two different views. The distance between the ad-molecule and the ribbon is indicated by the letter  $d$ . It is defined as the distance between the mean position of the heavy atoms in the ad-molecule and the plane of the ribbon. The supercell unit cell dimensions along the  $a$  and  $b$  axes are 3.0 and 1.8 nm, respectively, which is adequate to minimize the electrostatic interaction with the periodic images. Along the periodic cell, the dimension depends on the model study and is summarized in the Supporting Information for some of the models studied. For the case of seven subunits and without ad-molecule  $c = 1.727$  nm whereas with ad-molecule  $c = 1.728$  nm. In the case of 8-ZGNR with the ad-molecule  $d \approx 0.41$  nm.

We use localized pseudoatomic orbitals as implemented in the DFT program SIESTA for the electronic structure computation.<sup>8</sup> The geometry of the ribbon and ad-molecule is fully relaxed in a supercell with periodicity along the ribbon. Uniform

\* To whom correspondence should be addressed. E-mail: dalosto@intec.unl.edu.ar.

<sup>†</sup> University of Washington.

<sup>‡</sup> National Institute of Standards and Technology.

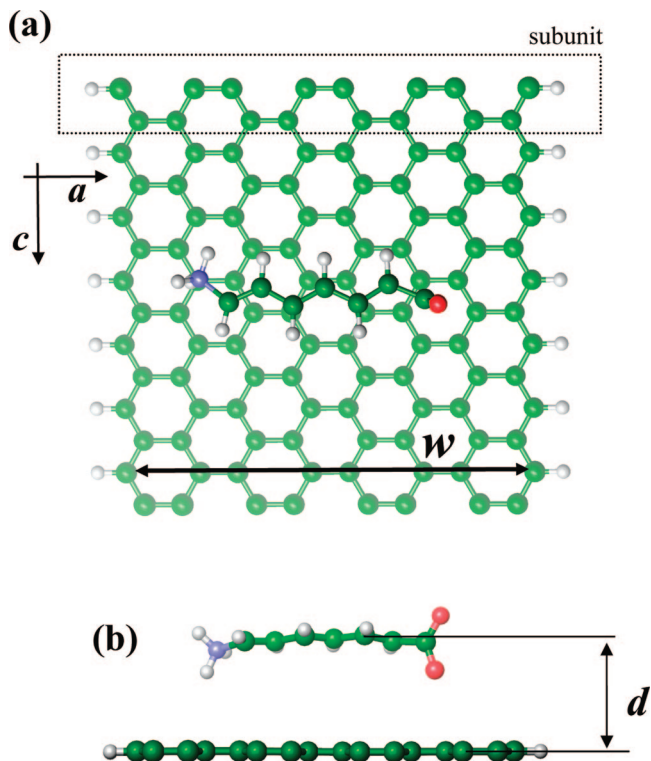


**Figure 1.** (a) Ball and stick model for 8-ZGNR with the short ad-molecule on the surface in a monohydrogenated supercell with green carbon atoms, grey hydrogen atoms, red oxygen atoms, and blue nitrogen atoms. The ribbon is periodic along the  $c$  axis. The rectangle indicates the subunits (seven subunits in this case). The width  $w$  is indicated. (b) Side view of the ribbon with the short ad-molecule separated by the distance  $d$ .

sampling of 12  $k$  points in a seven subunit supercell is employed to reach energy convergence which is approximately the same density of  $k$  points as 96  $k$  points needed for convergence in a single subunit.<sup>4</sup> The residual forces on the ribbon are less than 0.01 eV/nm, while the forces between the ribbon and the ad-molecule are less than 0.05 eV/nm. Double- $\zeta$  plus polarization (DZP) basis sets and optimized Troullier–Martins pseudopotentials are chosen for the computation.<sup>9</sup> For the exchange correlation energy we adopt the Perdew–Burke–Ernzerhof (PBE) version of the generalized gradient approximation (GGA) functional.<sup>10</sup> It was reported that using screened exact exchange density functional theory (HSE) better agreement was found between the experimental and theoretical gap than with LDA or PBE.<sup>4,11</sup> However, we think that the PBE functional can still describe changes in the band gap due to polar molecules. Since it was shown that the ground state for the graphene ribbons is the antiferromagnetic state (AF), we prepared the initial wave function to start the self-consistent solution with the spins oriented to reflect that state. We computed the total energies for the unpolarized and ferromagnetic cases (FM) to check our results. We found that the total energy for the unpolarized and FM cases is higher than the AF case, in agreement with earlier studies.<sup>5,12,13</sup>

Spin polarization studies using LSDA, GGA, and HSE showed that ZGNR has a finite band gap.<sup>4,14,15</sup> Recently, Yang et al.<sup>14</sup> calculated the band gap in ZGNR using the GW approximation, which gives superior estimates of the band gap in a range of systems.<sup>16,17</sup> They found that the GW correction (G, Green function; W, screened coulomb) changes the band dispersion, indicating a smaller effective mass and higher mobility for the carriers than the LSDA predictions. In particular,

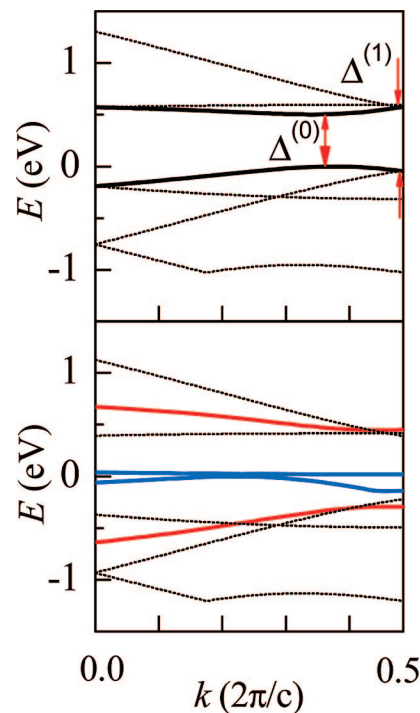


**Figure 2.** Spin-resolved band structure of the 8-ZGNR without  $E_{\text{ext}}$  (top) and with a uniform electric field  $E_{\text{ext}} = 2.0$  V/nm along the direction perpendicular to the edges (bottom). The energy of the top of the last occupied valence band is shifted to zero. The bands at the gap are shown with full lines, while the other bands are shown with dashed lines. The blue lines correspond to the bands for the  $\beta$ -spin state and red to bands for the  $\alpha$ -spin state. For this particular value of the electric field using the GGA, the  $\beta$ -spin gap is open by  $\Delta^{(0)} = 0.023$  eV.

the band gap for the case we are studying (8-ZGNR) is given in the different approximations as follows: LSDA  $\Delta^{(0)} = 0.3$  eV and  $\Delta^{(1)} = 0.5$  eV (ref 6 and this work), GGA  $\Delta^{(0)} = 0.5$  eV and  $\Delta^{(1)} = 0.9$  eV (this work), HSE  $\Delta^{(0)} = 1.1$  eV (refs 5 and 13), and LSDA-GW  $\Delta^{(0)} = 1.25$  eV and  $\Delta^{(1)} = 1.9$  eV (ref 14), where  $\Delta^{(0)}$  and  $\Delta^{(1)}$  are the direct band gap and energy gap at the zone boundary, respectively. The GW and HSE computation of the band gap suggest that the electric field necessary to close the gap is higher than the one computed within LSDA. Since we are using the GGA to study how the electric field produced by a polar molecule can be used for tailoring the band gap, our results should capture trends and underestimate the required electric field to create half metallicity by a factor of 2–3.

The top panel of Figure 2 shows the spin-resolved band structure of the 8-ZGNR in the absence of an external electric field. Our calculation of the band structure of the 8-ZGNR without an ad-molecule, calculated with a single subunit per unit cell, is nearly identical to that of ref 7. However, with a unit cell of seven subunits, the bands shown in Figure 2 appear with 7 times less dispersion due to the zone folding. The band structure reflects the antiferromagnetic ground state of the 8-ZGNR. In comparison, the band structure of the ferromagnetic ribbon includes a crossing of the lowest conduction band with the higher valence band.<sup>10</sup> In contrast, the spin-unpolarized calculation, which is not the ground state for the ZGNRs, presents 2-fold degenerate flat bands at  $E_F$ .<sup>7</sup>

Following the comparison with ref 7, the spin-resolved band structure of the 8-ZGNR using the GGA obtained with an electric field of 2.0 V/nm applied in the direction perpendicular to the edges is presented in the lower panel of Figure 2. The

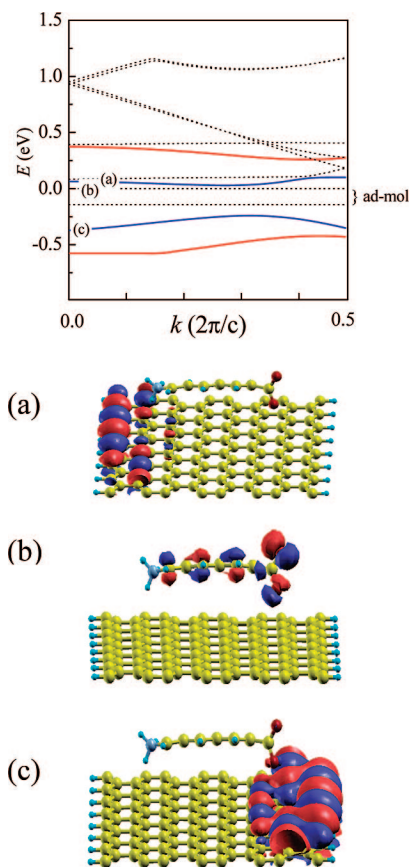


**Figure 3.** (top) Spin-resolved band structure of the 7-subunit 8-ZGNR with the short ad-molecule and without an electric field. The energy of the top of the highest last occupied valence band is shifted to zero. The  $\alpha$  spin is given in red lines, and the  $\beta$  spin is given in blue lines. (a–c) Orbitals calculated at the  $\Gamma$  point for the  $\beta$  spin for some state around the Fermi level. The bands between labels a and c have contributions primarily from the ad-molecule. (a and c) Orbitals of the  $\beta$  spin bands localized at the edge of the ribbon. (b)  $\beta$  spin orbital localized in the ad-molecule.

gap for the  $\alpha$  spin opens, while that for the  $\beta$  spin goes to zero (for  $E_{\text{ext}} = 2.0$  V/nm,  $\Delta^{(0)} = 24$  meV). The critical value of  $E_{\text{ext}}$  for which the gap closes in the GGA approximation is 2.1 V/nm, which is a bit larger than with LSDA with a value of 2.0 V/nm. At that point the ZGNR is metallic for  $\beta$ -spin electrons and semiconductor for  $\alpha$ -spin electrons. The dipole moment of the 8-ZGNR is 0 C m when  $E_{\text{ext}} = 0.80 \times 10^{-30}$  C m (14 D) with  $E_{\text{ext}} = 1.0$  V/nm and  $103 \times 10^{-30}$  C m (31 D) with  $E_{\text{ext}} = 2.0$  V/nm. Moreover, the GW and HSE calculation indicate that the  $E_{\text{ext}}$  necessary to close the band gap is 2–2.3 times the one obtained using GGA.

We are interested in tailoring the band gap in ZGNR through the electric field induced by polar molecules. For example, we imagine a device where the ribbon is immersed in a solution of molecules and some of these are polar molecules. With the band gap biased by an external field, it is still open for both spin states, but when a polar molecule moves close to the ribbon, it closes and a polarized spin current could be induced with an electric field along the edges of the ribbon. Thus, we located a polar molecule on the surface of the 8-ZGNR, shown in Figure 1. After complete relaxation of the system we computed the spin-resolved band structure which is presented in Figure 3 for the case of the 8-ZGNR with the short ad-molecule. The ad-molecule produces the same response in the 8-ZGNR as an external electric field of  $\sim 1.0$  V/nm, which corresponds to an intermediate value between 0 (semiconductor for  $\alpha$  and  $\beta$  spin)

and 2.1 V/nm (semiconductor for  $\alpha$  spin and metallic for  $\beta$  spin). The bands of  $\alpha$  spin open, while the bands for  $\beta$  spin reduce their band gap, see Figure 3. Between the  $\beta$ -spin bands there are two spin-degenerate bands predominantly localized on the ad-molecule. In addition, these bands show no wavevector dependence. The  $\beta$ -spin band gap for the 8-ZGNR with the ad-molecule on the surface is 0.27 (46% reduction) and 0.15 eV (70% reduction) with the short and long ad-molecule, respectively. Some states localized in the ad-molecule contribute to the bands around the Fermi energy. Panel b in the lower part of Figure 3 shows the  $\beta$  spin for one of these states localized in the ad-molecule. The  $\alpha$  spin is similar and not shown here. Since we are interested in the bands which correspond to the edges of the ribbon, we analyze the contributions from the ribbon and from the ad-molecule to the bands around the Fermi level. The lower part of Figure 3, panels a and c, shows the calculated orbitals at the  $\Gamma$  point for the bands relevant to define the band gap. Recall that with our seven-subunit supercell the  $\Gamma$  point corresponds to seven uniformly spaced  $k$  points in the band structure of the one-subunit ZGNR system. The edge states and states of the ad-molecule show little mixing. Although the electric field due to the ad-molecules on the ribbon is not uniform on the ribbon surface, it is still capable of changing the band gap as a uniform electric field does. The band structure and orbitals for the case of the ribbon with the long ad-molecule are qualitatively similar to the ones presented in Figure 3 for the short ad-molecule, and it is not presented here. The results presented were computed using a static picture of the ribbon and ad-molecule, and it is certainly possible that the fluctuations in the position of the ad-molecule with respect to the ribbon spread the band-gap values. To understand the potential-energy surface (PES) and binding energy between the 8-ZGNR and the ad-molecule we computed the PES for the ad-molecule around the equilibrium position but without relaxation. We choose the short ad-molecule for that study. Displacement of the short ad-molecule  $\pm 0.05$  nm along the  $a$  axis or  $c$  axis, Figure 1 (corresponding to displacements parallel to the surface of the ribbon), implies a change in the total energy of 3 and 0.2 meV, while displacement  $\pm 0.05$  nm along the  $b$  axis (corresponding to a displacement perpendicular to the ribbon) is 180 meV. Hence, at room temperature there could be important position fluctuations along the directions parallel to the ribbons and more confined in the perpendicular direction. However, the band gap changes less than 10 meV. In addition, the van der Waals forces, not considered in the present computation, could modify the position of the ad-molecule with respect to the ribbon by about 0.05 nm based on results in the other organic systems.<sup>18</sup> Such a change in position would change the band gap by a few millielectronvolts.

It is interesting to correlate the value obtained for the gap in the presence of the ad-molecule with the corresponding  $E_{\text{ext}}$  which produces the same band gap. Figure 4 shows the dependence of the gap as a function of  $E_{\text{ext}}$  using LSDA and GGA for the 8-ZGNR with and without the ad-molecule. The square symbols represent different unit cell dimensions for the 8-ZGNR with the short ad-molecule. The square symbol numbered 7 corresponds to the system shown in Figure 1 with seven subunits along the  $c$  axis of the 8-ZGNR. We reduced the unit cell dimensions from seven subunits to six and four subunits to study the effect of increasing the density of ad-molecules on the band gap. We find the band gap decreases substantially as the density of ad-molecules is increased, see Figure 4. The star symbol shown in Figure 4 corresponds to the 8-ZGNR with the long ad-molecule. Increasing the dipole

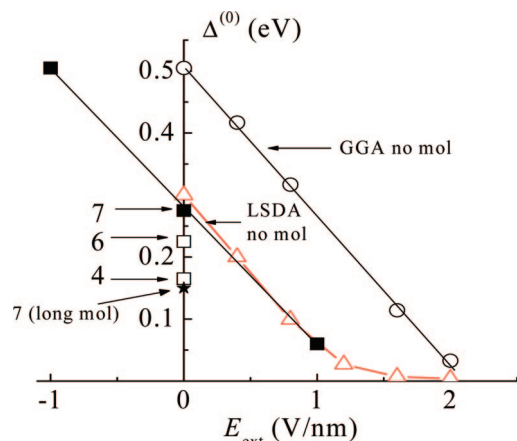


**Figure 4.** Direct band gap for the  $\beta$ -spin state as a function of  $E_{\text{ext}}$ . Open triangles are LSDA calculations, while all other calculations use the GGA. The closed squares labeled 7 and the open squares labeled 6 and 4 correspond to the number of subunits in the supercell calculation of 8-ZGNR including the short ad-molecule (see text for details). The star corresponds to the 7-subunit 8-ZGNR with the long ad-molecule.

moment of the ad-molecule (long ad-molecule/short ad-molecule  $\approx 1.5$ ) has the same effect on the band gap as reducing the cell dimension of the 8-ZGNR to four subunits, as shown in Figure 4.

Also in Figure 4 we study the addition effect of the external electric field and the field produced by the ad-molecule. In this case, the computation of the band gap was carried out without relaxation of the system. The band gap computed for the 8-ZGNR with the short ad-molecule and also in the presence of an  $E_{\text{ext}} = 1.0$  V/nm (corresponding to the positive  $a$  axis in Figure 1a) in the antiparallel direction of the dipole moment of the ad-molecule gives a similar band gap ( $\sim 0.50$  eV) to that when  $E_{\text{ext}} = 0$  and without the ad-molecule. Thus, the external electric field cancels out approximately the electric field due to the ad-molecule. The dipole moment of the system is  $\sim 20 \times 10^{-3}$  C m (3.6 D), four times smaller than when  $E_{\text{ext}} = 1.0$  V/nm. A different situation occurred when  $E_{\text{ext}} = -1.0$  V/nm is applied along the negative  $a$  axis, in the parallel direction of the dipole moment of the short ad-molecule, the  $\beta$ -spin band gap is almost closed with  $\Delta^{(0)} \approx 0.06$  eV similar to the case of  $E_{\text{ext}} = 1.8$  V/nm, without the ad-molecule. Besides, the total energy of this configuration ( $E_{\text{ext}}$  antiparallel to the ad-molecule dipole moment) is lower than the first one ( $E_{\text{ext}}$  parallel to the ad-molecule dipole moment).

On the basis of the shape of the LSDA and GGA results in the linear region when an external field is applied and the gap computed using GW<sup>14</sup> and HSE<sup>5,13</sup> functional without external electric field, we estimate the value of  $E_{\text{ext}}$  necessary to close the gap at 5 V/nm. The PBE functional underestimates the band gap by more than two times with respect to GW or HSE computations. However, the important point is that the band gap could be biased with an external electric field, and then the band gap could be modulated, possibly even closed, in the presence of polar molecules.

We showed using first-principles calculations that the gap of a ZGNR can be modulated by the presence of the electric field due to a polar molecule. This is an interesting result which may be used to design a sensor. Although using the GW and screened exact exchange HSE functional computation of the band gap<sup>13,4</sup> suggests that the electric field necessary to close the gap will be substantially higher than the one computed with GGA, the important point is that the band gap could be biased with an external electric field and for the presence of polar molecules. In addition, the van der Waals forces, not considered in our computation, would change the band gap by a few millielectronvolts. Moreover, the presence of polar ad-molecules affects the band gap in the same way  $E_{\text{ext}}$  does.

**Acknowledgment.** This work was supported in part by NIST Grant 70 NAMB 2H003 and DOE Grant DE-FG03-97ER45623 and facilitated by the DOE Computational Materials Science Network. We thank Prof. Steven G. Louie for providing the input to the SIESTA code for the case of one subunit. Computing was performed at NIST's Raritan cluster.

**Supporting Information Available:** Structure of the 8-ZGNR with the short ad-molecule shown in Figure 1. This material is available free of charge via the Internet at <http://pubs.acs.org>.

## References and Notes

- (1) (a) Novoselov, K. S.; Geim, A. K.; Morozov, S. V.; Jiang, D.; Zhang, Y.; Dubonos, S. V.; Grigorieva, I. V.; Firsov, A. A. *Science* **2004**, *306*, 666. (b) Novoselov, K. S.; Jiang, Z.; Zhang, Y.; Morozov, S. V.; Stormer, H. L.; Zeitler, U.; Maan, J. C.; Boebinger, G. S.; Kim, P.; Geim, A. K. *Science* **2007**, *315*, 1379.
- (2) (a) Chen, Z.; Lin, Y.-M.; Rooks, M. J.; Avouris, P. *Physica E* **2007**, *40*, 228. (b) Han, M. Y.; Özyilmaz, B.; Zhang, Y.; Kim, P. *Phys. Rev. Lett.* **2007**, *98*, 206805.
- (3) Ezawa, M. *Phys. Rev. B* **2006**, *73*, 045432.
- (4) Barone, V.; Hod, O.; Scuseria, G. E. *Nano Lett.* **2006**, *6*, 2748.
- (5) Hod, O.; Barone, V.; Peralta, J. E.; Scuseria, G. E. *Nano Lett.* **2007**, *8*, 2295.
- (6) Son, Y.-W.; Cohen, M. L.; Louie, S. G. *Phys. Rev. Lett.* **2006**, *97*, 216803.
- (7) Son, Y.-W.; Cohen, M. L.; Louie, S. G. *Nature (London)* **2006**, *444*, 347.
- (8) Soler, J. M.; Artacho, E.; Gale, J. D.; Garcia, A.; Junquera, J.; Ordejon, P.; Sanchez-Portal, D. *J. Phys.: Condens. Matter* **2002**, *14*, 2745.
- (9) Troullier, M.; Martins, J. L. *Phys. Rev. B* **1991**, *43*, 1993.
- (10) Perdew, J. P.; Burke, K.; Ernzerhof, M. *Phys. Rev. Lett.* **1996**, *77*, 3865.
- (11) (a) Heyd, J.; Scuseria, G. E.; Ernzerhof, M. *J. Chem. Phys.* **2003**, *118*, 8207. (b) Heyd, J.; Scuseria, G. E. *J. Chem. Phys.* **2004**, *120*, 7274.
- (12) Pisani, L.; Chang, J. A.; Montanari, B.; Harrison, N. H. *Phys. Rev. B* **2007**, *75*, 64418.
- (13) Hod, O.; Barone, V.; Scuseria, G. E. *Phys. Rev. B* **2007**, arXiv: cond-mat/0709.0938.
- (14) Yang, L.; Park, C.-H.; Son, Y.-W.; Cohen, M. L.; Louie, S. G. *Phys. Rev. Lett.* **2007**, *99*, 186801.
- (15) Barone, V.; Hod, O.; Scuseria, G. E. *Nano Lett.* **2006**, *6*, 2748.
- (16) Aulbur, W. G.; Jonsson, L.; Wilkins, J. W. *Solid State Phys.* **2000**, *54*, 1.
- (17) (a) Hybertsen, M. S.; Louie, S. G. *Phys. Rev. B* **1986**, *34*, 5390. (b) Hybertsen, M. S.; Louie, S. G. *Phys. Rev. Lett.* **1985**, *55*, 1418. (c) Shirley, E. L.; Terminello, L. J.; Klepeis, J. E.; Himpfel, F. J. *Phys. Rev. B* **1996**, *53*, 10296.
- (18) (a) Chakarova, S. D.; Schroeder, E. *J. Chem. Phys.* **2005**, *122*, 054102. (b) Rydberg, H.; Dion, M.; Jacobson, N.; Schroder, E.; Hyldygaard, P.; Simak, S. I.; Langreth, D. C.; Lundqvist, B. I. *Phys. Rev. Lett.* **2003**, *91*, 126402.